Comparison of Statistical and Deterministic Smoothing Methods to Reduce the Uncertainty of Performance Loss Rate Estimates

Philip Ingenhoven, Giorgio Belluardo, and David Moser

***Abstract*—With the large increase of installed photovoltaic (PV) capacity introduced in the energy system, one aspect that becomes increasingly important is the long-term reliability of the energy output and, thus, the estimation of the performance loss rate (PLR) for the different technologies on the market. Reliable performance metrics and statistical methods are needed to exploit continuous outdoor measurements, in order to assess the long-term performance and, thus, the financial viability of solar PV systems, as well as their long-term stability as an important part of the energy mix. This paper presents and compares seven different methodologies to extract reliable long-term performance indicators from monitored field data. The methods can be grouped into four different approaches. First, a simple computation of the performance ratio (PR) is used as a benchmark for the other methods. Second, these PR values are fitted to two sinusoidal functions that emulate the climatic influence and a decaying trend that represents the degradation of the PV array. Third, two kinds of time-series decomposition [namely classical series decomposition and seasonal-trend decomposition based on local regression (STL)] are applied, and the trend is linearized to find the PLR. Finally, two methods are presented that aim to utilize the physical properties of the material to correct for seasonal fluctuations, namely the correction to standard test conditions of the PR via normal operating conditions (PR_{NOCT}) and a performance metric called array photovoltaic for utility system applications (PVUSA). In this work, the degradation rates from the different computational methods are presented. The main focus is on the understanding of the uncertainty associated with each of the methods. All the methods yield comparable results; however, the statistical time-series methods deliver the highest accuracy in almost all the investigated cases, especially for technologies affected by metastable effects. On average, the two periodic methods halve the uncertainty and the time-series methods reduce the uncertainty, on average, to 45%, whereas the methods PR_{NOCT} and PVUSA reduce to only 75% of the benchmark method. Methods that are trying to incorporate the module physics (PR_{NOCT} and PVUSA) work best to reduce the uncertainty only for technologies, in which the temperature behavior is well known, i.e., crystalline-silicon-based modules. For this reason, the usage of the STL method for the computation of the PLR is proposed.**

***Index Terms*—Performance loss rate (PLR), performance ratio (PR), photovoltaic (PV) degradation, time-series smoothing, uncertainty analysis.**

Manuscript received May 11, 2017; revised July 11, 2017 and September 11, 2017; accepted October 8, 2017. Date of publication November 15, 2017; date of current version December 20, 2017. *(Corresponding author: Philip Ingenhoven.)*

The authors are with the Institute for Renewable Energy, European Academy of Bozen/Bolzano (EURAC Research), 39100 Bolzano, Italy (e-mail: philip.ingenhoven@eurac.edu; giorgio.belluardo@eurac.edu; david.moser@eurac.edu).

Color versions of one or more of the figures in this paper are available online at http://ieeexplore.ieee.org.

Digital Object Identifier 10.1109/JPHOTOV.2017.2762523

I. Introduction

PHOTOVOLTAIC (PV) energy production will play a major role in the future energy mix. By the end of 2016, a total worldwide power of 296 GW was reportedly installed [1]. The steadily rising efficiency together with the continued fall of production costs is enhancing this trend. Simultaneously, new technologies and industrial processes ensure an ever higher level of reliability of the PV products. This is a key factor for the evaluation of financial viability of an investment into the PV energy production. The performance loss rate (PLR) is one of the input information necessary to estimate the long-term energy yield of a future PV plant in the design phase. Thus, a wrong value of the predicted PLR for calculation might lead to an overestimation or to an underestimation of the future actual value of the exceedance probability P50, P90 and of the levelized cost of electricity. The PV plant might, thus, not accomplish a minimum energy yield if guaranteed by the operation and maintenance contract or the business plan can be weaker that it really is, and the project might not be sufficiently attractive to investors [2]. On the module manufacturers' side, there is the need to collect as much data as possible on the PLR over the first 25 years of the lifetime of their products, in order to tune the warranties to more competitive levels. In fact, in the future, warranties might be even provided according to the climate of the installation site. This is the result of the actual switch from a power rating attitude [power output measured in the laboratory under standard test conditions (STCs)] to an energy rating attitude (i.e., performance assessment based on the energy output under real operating conditions) for the performance assessment of a PV module [3], [4]. This switch of paradigm is actually demonstrated by the ongoing development of a new part of the IEC 61853 standard (IEC 61853-3) on the energy rating of PV modules by the International Electrotechnical Commission (IEC) Technical Committee 82 Working Group 2 (IEC/TC82/WG2) [5], [6]. The reduction of uncertainties from these estimates is vital for investors as well as for PV module manufacturers. Hence, there is the need to define standardized procedures on how to monitor and assess the performance and degradation of the modules and to collect field data from different technologies under different climatic conditions and relate these to the results of accelerated ageing tests.

The reasons for PV degradation are continuous cycles of temperature, humidity, irradiation, mechanical stress, spotted

soiling that can induce corrosion of the metallic connections, delamination, discoloration and breakages of the module, cracks of the cells, hot spots, bubbles, and other failures [7]–[10]. In addition to material degradation, a PV module or array under outdoor operating conditions is exposed to other factors directly acting on its electric performance. These are diffuse soiling, snow, shading, modules, and cell mismatch. For this reason, it is, therefore, more appropriate to speak about the PLR rather than the degradation rate, as already stated in [11]. The PLR of a PV module or a system depends on the PV technology, the local climatic condition, and to an non-negligible extent on the method and experimental setup used to assess and collect the data. The PLR can be determined in principle in two ways: indoor measurements [10], [12], [13] and outdoor measurements [14]–[18].

In recent years, numerous studies have been published on this topic. In an overview study, Jordan *et al.* [19] analyzed 11 000 degradation rates in almost 200 studies from 40 different countries, where a median degradation for x-Si technologies in the 0.5–0.6% per year range with the mean in the 0.8–0.9% per year range was found. Heterointerface technology (HIT), microcrystalline silicon (μc-Si), and other thin-film technologies were found to exhibit degradation around 1% per year. A further study using the same database [20] found the short-circuit current (I_{sc}) and, to a lesser extent, the fill factor (FF) to be the largest contributors to power degradation. A long-term study [21] analyzed the performance of 204 crystalline-silicon-based modules installed in the 1980s over about 19–23 years, showing an average of 0.8% per year PLR, with 82.4% of modules respecting the typical manufacturers' warranty.

For the calculation of the PLR from field measurements, a performance metric and a statistical method have to be defined. A performance metric consists in an analysis technique to calculate representative performance estimators. Among these, the array performance ratio (PRa) and array photovoltaic for utility system applications (PVUSA) indexes are the most common ones [22]. The statistical methods are mathematical algorithms applied on the time series of performance estimators in order to extract a trend. The most common is linear regression, as well as classical series decomposition (CSD) [23], [24], locally weighted scatter-plot smoothing (seasonal-trend decomposition using local regression—STL) [25], [26], and autoregressive integrated moving average (ARIMA) [27].

To find an accurate estimate of the PLR, it is necessary to find methods, i.e., a combination of a performance metric and a statistical method, which succeed in minimizing seasonal oscillation and eliminate outliers. There are two main strategies to achieve this. A first group of methods are the so-called *deterministic methods*, which correct the performance metric to some reference conditions, in an attempt to eliminate seasonality. A successful correction of the performance metric presumes the knowledge of the seasonal behavior of a PV system, which, in turn, is the result of several effects due to the changing ambient conditions (irradiance, temperature, wind speed and direction, and solar spectrum) and to the intrinsic characteristics of the material itself (metastable effects such as Staebler–Wronski and light soaking; see, e.g., [28]). The second strategy applies a *statistical smoothing* in an attempt to extract a seasonality and a long-term trend from the time series of a generic performance metric. This last group of methods does not require a deep knowledge of the ambient effects on PV technologies and of the material, but it treats a PV system simply as a black box whose output is modeled in a statistical way. Many studies developed, compared, and analyzed the PLR using deterministic smoothing [11], [29]–[32]. On the other hand, methodologies based on statistical smoothing have been developed only recently [17], [33]–[36]. A comprehensive review of all methodologies belonging to the two described groups is reported [37], where trends in PLR values and accuracy are also extracted. In this study, a strong accent is put on the need for further exploitation of outdoor measurements to compare the results and the accuracy of these methodologies in multiple locations.

The scope of this paper is to use established performance metrics and to apply both deterministic and statistical smoothing techniques to analyze the PLR over six years of operation of 26 different PV systems representing eight different PV technologies installed in the Alpine environment of Bolzano, in the north of Italy.

In particular, the performance metrics used here are: PRa (shortened in the following as PR) and a PR that is corrected to the nominal operating temperature of the modules PR_{NOCT} as well as PVUSA. The statistical smoothing methods will be applied to the PR metric, namely a simple regression, fitting to periodic functions as well as classical and STL time-series decomposition. The methods are described in full detail in Section III-B.

The 26 tested PV module types are grouped in eight distinct technologies, listed in the following. This paper is structured as follows. In Section II, the experimental setup is presented. In Section III, seven methods to extract the PLR are discussed in detail. In Section IV, the results are presented. The results are discussed in Section V.

II. Experimental Setup

The data analyzed in this paper were collected from the PV outdoor test facility of Airport Bolzano Dolomiti (position ca. 46.46N, 11.33E, elevation: 262 m) located in South Tyrol, Italy [38]. The facility is located at the junction of the three valleys: Val d'Isarco, Val Sarentino, and Val d'Adige, and its climate is classified as *Cfb* (temperate, without dry season, warm summer) according to Köppen classification [39]. Average monthly precipitation in winter in the analyzed period was 37.5 mm, in spring 58.5 mm, in summer 85.1 mm, and in autumn 84.8 mm according to historical data measured by the province [40]. Furthermore, the average daytime temperatures in summer were 25 °C with a maximal temperature of 40 °C reached, average daytime winter temperatures reached were 5 °C with a minimum night temperature of −11 °C measured in our weather station. Twenty-six PV arrays from 1 to 7 kWp of different module types (technology, manufacturer, and design) are installed at a fixed tilt of 30° and an orientation of 8.5° West of South. The main characteristics of the arrays and of the modules are summarized in Table I. All arrays are installed within 100 m of

TABLE I
MAIN CHARACTERISTICS OF INVESTIGATED PV ARRAYS

Tech	N –	P_{mod} W	P_{tot} kW	T_{coef} %/K	NOCT °C	η_{mod}	Inverter Type	Module
1j-a-Si1	20	50	1	− 0.19	46	5%	SB1100	frameless glass–glass
1j-a-Si2	12	100	1.2	− 0.20	49	7%	SB1100	framed glass–foil
2j-a-Si1	36	27	0.97	− 0.20	46	5%	SB1100	frameless glass–glass semitransparent
3j-a-Si1	3.5	272	0.95	− 0.21	46	6%	SB1100	solarlaminat on iron sheet
3j-a-Si2	3.5	272	0.95	− 0.21	46	6%	SB1100	solarlaminat on iron sheet
CdTe2	90	77.5	6.98	− 0.25	45	11%	SMC7000TL	frameless glass–glass
CIGS2	20	55	1.1	− 0.25	46	7%	SB1100	framed glass–glass
CIGS3	14	80	1.12	− 0.36	47	11%	SB1100	framed glass–glass
CIGS4	14	80	1.12	− 0.36	47	11%	SB1100	framed glass–glass
HIT1	18	215	3.87	− 0.30	48	17%	SB4000TL	framed glass–foil
c-Si1	14	140	1.96	− 0.50	45	11%	SB4000TL*	frameless glass–glass back contact
c-Si2	16	124	1.98	− 0.50	45	13%	SB4000TL*	frameless glass–glass opaque
c-Si3	8	220	1.76	− 0.50	45	13%	SB4000TL*	framed glass–foil
c-Si4	4	300	1.2	− 0.38	45	18%	SB1100	framed glass–foil back contact
c-Si5	4	300	1.2	− 0.38	45	18%	SB1100	framed glass–foil back contact
micro1	10	110	1.1	− 0.25	48.4	8%	SB1100	frameless glass–glass
micro2	10	115	1.15	− 0.25	46	8%	SB1100	frameless glass–glass
micro3	8	135	1.08	− 0.24	48	9%	SB1100	framed glass–foil
mc-Si1	18	222	4	− 0.43	45	14%	SB4000TL	framed textured front glass–foil
mc-Si2	18	230	4.14	− 0.45	45	14%	SB4000TL	framed glass–foil
mc-Si3	24	175	4.2	− 0.44	46.9	14%	SB4000TL	framed glass–foil
mc-Si6	20	210	4.2	− 0.457	49	14%	SB4000TL	framed glass–foil
mc-Si7	11	225	2.48	− 0.50	47.9	14%	SB4000TL*	framed glass–foil
mc-Si8	9	225	2.03	− 0.45	47	13%	SB4000TL*	framed glass–foil
mc-Si9	9	230	2.07	− 0.45	47	14%	SB4000TL*	framed glass–foil
ribbon1	20	205	4.1	− 0.45	44.8	13%	SB4000TL-20	framed glass–foil

Nominal power per module (P_{mod}) and total array (P_{tot}), temperature coefficient (T_{coef}) and nominal operating cell temperature (NOCT) from the data sheet, module efficiency η_{mod}, important module characteristics (Module Type), and the inverter type are also indicated. All inverters are SMA Sunny Boy models (*Two systems connected to one inverter with two separate MPP tracking devices).

the weather station and are exposed to similar horizon shading; however, due to self-shading of the rows, some modules experience local shading in December. DC-side electrical parameters of each array are measured every 15 min by commercial inverters (SMA; see Table I for details) ensuring a good level of accuracy in current (I_{mpp}) and voltage (V_{mpp}), with an average difference from a dedicated system of less than 5% and less than 2%, respectively, decreasing at higher irradiance [41], [42]. The inverters are all from the same manufacturer (see Table I), and errors due to different maximum power point (MPP) tracking are assumed to be comparable between the different systems. Thus, the PLRs are deducible from the data collected this way. A dedicated meteo station collects data of global horizontal, direct normal, and diffuse horizontal irradiance, as well as global plane-of-the-array (POA) irradiance. Furthermore, wind speed and ambient temperature are measured. The acquisition frequency is 1 min, which is then averaged on a 15-min time interval to match the electrical data. The sensors are systematically cleaned and periodically calibrated in order to comply with the standard IEC61724:1998 [43]. Electrical data have been recorded since August 2010, while weather data are available from February 2011. The abbreviations used for the different technologies are the following: namely single/double/triple junction amorphous silicon (1/2/3a-Si), cadmium telluride (CdTe), copper indium gallium selenide (CIGS), heterojunction solar cells (HIT), monocrystalline silicon (c-Si), micromorphous silicon (micro), poly/multicrystalline silicon (mc-Si), and polycrystalline silicon string Ribbon (ribbon). In contrary to our earlier papers (see, e.g., [11] and [38]), we used c-Si for monocrystalline instead of mc-Si and mc-Si poly/multicrystalline silicon instead of pc-Si.

III. METHODS

In this section, we describe the seven different methods used to compute the PLR, namely:

1) linear regression (over full years) of the uncorrected PR;
2) fitting of the uncorrected PR with single and double periodic functions;
3) classical time-series decomposition on the uncorrected PR;
4) STL decomposition of the uncorrected PR;
5) linear regression of the corrected PR (to STCs);
6) linear regression of PVUSA.

The first method is the most straightforward approach, using linear regression only on the measured data. The methods using periodic fitting try to catch the seasonal influence of insolation, spectral variation, and temperature. The methods using time-series decomposition are purely statistical, whereas the last two methods aim to use the physical properties of the modules in more detail. The methods will be described in detail in Section III-B.

A. Preliminary Filtering

All data are filtered to exclude obvious outliers caused by different irradiance conditions at the pyranometer and the PV

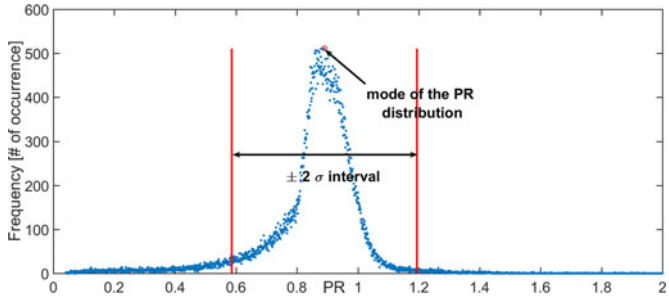

Fig. 1. Histogram of all measured 15-min values of the PR of c-Si1. Outlier are filtered out using the $\pm 2\sigma$ interval around the most likely PR value. PR values above 1 are due to low temperatures in the winter at which crystalline silicon modules perform better than at STCs. The asymmetry toward lower PR values can be seen in all analyzed technologies and indicates that the PR is not normally distributed, i.e., it is more likely for a PV system to underperform than it is to overperform.

array (e.g., due to local shading) or other malfunctions in the monitoring system. First, the 15-min PR is computed for the complete dataset of each technology as follows:

$$\mathrm{PR}(t) = \frac{P_{\mathrm{DC}}(t) \cdot G_{\mathrm{STC}}}{G_{\mathrm{POA}}(t) \cdot P_n} \tag{1}$$

where $P_{\mathrm{DC}}(t)$ is the power value of the PV array at time t, $G_{\mathrm{POA}}(t)$ is the irradiance on the POA at time t, $G_{\mathrm{STC}} = 1000\,\mathrm{W/m^2}$ is the reference irradiance, and P_n is the nominal power of the array, as reported in Table I. The most likely PR value, i.e., $\mathrm{PR}_{\mathrm{mode}}$, is identified, and a filter with a width of $\pm 2\sigma$ is created around it, excluding all values falling out of this range (see Fig. 1). The filter developed here was compared with the usage of local shading filters on several systems that are affected by a different local shading than the weather station. The resulting monthly PR values of both filtering methods were comparable. For nine of the technologies, local shading diagrams were available and tested. The resulting difference in the PLR amounted to 0.03% on average with a maximum difference of 0.07%. With these filtered values, the monthly values for the statistical methods are computed. For the physical methods (PR corrected and PVUSA), more filters are applied that will be described in the following.

The $\mathrm{PR}_{\mathrm{month,\,AC}}$ over a specified period is defined in the IEC 61724 standard [43] as the ratio of the final yield Y_f and the reference yield Y_r over that period. The different yields are defined as

$$Y_f = \sum_{\mathrm{month}} \frac{P_{\mathrm{AC}}(t)}{P_n},\; Y_r = \sum_{\mathrm{month}} \frac{G_{\mathrm{POA}}(t)}{G_{\mathrm{ref}}},\; Y_a = \sum_{\mathrm{month}} \frac{P_{\mathrm{DC}}(t)}{P_n} \tag{2}$$

where Y_a is the array yield, i.e., the generated dc energy per kilowatt of the installed PV array. For the purposes of this paper, only the dc energy is used in place of ac energy, thus leading to a slightly modified version of the PR, given by

$$\mathrm{PR}_{\mathrm{month,\,DC}} = \frac{Y_a}{Y_r}. \tag{3}$$

This definition makes sure that only effects of the PV arrays are taken into account. In the above-mentioned definition of $\mathrm{PR}_{\mathrm{month,\,AC}}$, as defined in [43], effects due to possible inverter degradation influence the results, hence the usage of (3). The period over which the PR was computed is one month. Shorter time periods show larger oscillations, and a yearly period does not allow a seasonal analysis; thus, the monthly evaluation period for the PR was chosen as a compromise.

B. Detailed Description of the Models

1) Linear Regression on the Uncorrected Performance Ratio: This method is used as a common benchmark for the other methods. The PR computed in (3) is used as a performance metric. The PR data are fitted to

$$\mathrm{PR}_{\mathrm{lin}}(t) = a \cdot t + b \tag{4}$$

where a (month^{-1}) is the gradient, and b is the dimensionless y-intercept of the linearized PR time series. The PLR (year^{-1}) is computed as

$$\mathrm{PLR} = \frac{12a}{b} \tag{5}$$

with the uncertainty of

$$u_{\mathrm{PLR}} = \sqrt{\left(\frac{12}{b}\right)^2 \cdot u_a^2 + \left(\frac{12a}{b^2}\right)^2 \cdot u_b^2} \tag{6}$$

where the uncertainties of the fitting constants ($u_{a/b}$) are taken from the curve-fitting toolbox of MATLAB [44]. Due to the changes in irradiance and temperature over the year and the physical response of the PV devices to these factors, $\mathrm{PR}_{\mathrm{monthly}}$ is a highly seasonal quantity, and the regression fit carries, therefore, an uncertainty that corresponds to the seasonality of the data. In the following sections, six methods are described to reduce these seasonal oscillations or separate these fluctuations from the long-term trends.

In the literature, two definitions, namely $\mathrm{PLR} = 12a$ (absolute; see, e.g., [35]) and $\mathrm{PLR} = \frac{12a}{b}$ (relative; see, e.g., [11]), are used, where a and b are the respective fitting coefficients of the linear regression. In all the methods presented here, the PLR is computed as the relative PLR, as defined in (5). The relative PLR makes it easier to generalize the findings to the energy yield of the array using the initial yield of the plant. This simplifies the usage of this value, for example, in setting up business models for future PV installations. Furthermore, it allows the direct comparison with the method PVUSA.

2) Fit to a Single and Double Periodic Functions: In the geographical latitude between the polar circles and the tropical circles, the solar insolation on the global horizontal plane follows more or less a sinusoidal function with a period of one year. To account for the shortcomings of the single periodic approximation and to incorporate the effect of temperature, we propose to use a fitting function with two sinusoidal periods. We additionally introduce an oscillation with twice the frequency. Therefore, we can estimate the seasonality of the PR values to follow this behavior and fit $\mathrm{PR}_{\mathrm{monthly}}$ with a single or double

periodic function as

$$\begin{aligned} \mathrm{PR}_\tau = \; & A_0 \cdot \sin\left(\frac{t}{\tau}\right) + B_0 \cdot \cos\left(\frac{t}{\tau}\right) \\ & + A_1 \cdot \sin\left(\frac{2t}{\tau}\right) + B_1 \cdot \cos\left(\frac{2t}{\tau}\right) \\ & + a \cdot t + b \end{aligned} \tag{7}$$

where $\tau = 12$. In the single periodic case, only the first two terms and the decaying trend are taken into account, whereas in the double periodic case, the whole equation is used. This estimation will break down outside the geographical latitude mentioned above. North of the Arctic (and south of the Antarctic) circle, the sun completely disappears for a period of time, where between the tropical circles, the insolation has two maximal within one year, which is miscaptured in the double periodic case. The PLR is now computed with just the linear part of the fitting function using (5), and the uncertainty is computed analogously to (6).

3) Classical Series Decomposition and Local Regression Methods: In the following two sections, the time-series decomposition methods are described. Both methods decompose the original $\mathrm{PR}_{\mathrm{monthly}}$ time series into three parts as follows:

$$\mathrm{PR}_{\mathrm{monthly}}(t) = T_t + S_t + R_t \tag{8}$$

where T describes the long-term trend of the time series, S the seasonality, and R the remainder. For the classical additive series decomposition, the trend T_t is found using a symmetrical 12-month moving average. The seasonality and the remainder are found following [24]. Due to the usage of the moving average to find the trend, the time series misses six months in the beginning and the end of the time series, leaving the trend series 12 months shorter than the original series.

To overcome the disadvantage of the shortened trend in the CSD, methods such as the ARIMA and the STL can be used to find an estimation of the trend also for the first and last six months of the time series, as, for example, done in [35]. In this work only the STL method [25] is considered. It would be possible to also use ARIMA algorithms; however, the main difference between the two methods is that ARIMA is specifically written for economic analysis and STL is more general. The STL method uses various loops of local regression using locally weighted scatter-plot smoothing; for details, see [24] and [25]. A linear fit as in (4) is used on the trend to define the performance loss estimation for both time-series decompositions. The PLR is estimated analogously to (5) from the fitting parameters. Both the classical and STL decompositions were performed using the time-series package [45] of the software R [46].

4) Performance Ratio Corrected for Temperature to Standard Test Conditions: The PR metric is corrected to the STC temperature of 25 °C. This method is described in detail in [11]. A temperature correction is performed on the 15-min-based values of P_{DC} using calculated values of back-of-module temperature and temperature coefficient from the modules' datasheet, using normal operating conditions (NOCT). Next, the monthly values of the metric $\mathrm{PR}_{\mathrm{NOCT}}$ are calculated using (2), and a linear regression is performed. This technique also involves a filtering step to exclude all measurements corresponding to an irradiance level lower than G_{POA} below 800 W/m^2, in order to reduce the uncertainty in the estimation of the PLR [11]. However, this way, a value of monthly $\mathrm{PR}_{\mathrm{NOCT}}$ cannot be calculated for one or more months during winter for the lack of a sufficient number of validated measurements. Compared with the linear regression on the uncorrected PR, this method is able to minimize also temperature effects, which play an important role especially for technologies, typically silicon based, with a high value of power temperature coefficient γ.

5) Photovoltaic for Utility System Applications: The PVUSA method allows a smoothing of the time series by reporting the values of performance over a specific period to the so-called *PV systems under performance test conditions* [47]: irradiance $G_{\mathrm{POA}} = 1000\ \mathrm{W/m^2}$, ambient temperature $T = 20\ ^\circ\mathrm{C}$, and wind speed $W = 1\ \mathrm{m/s}$. This method is described in detail in [11]. A value of PVUSA is calculated for each month using computed parameters, and a linear regression is then performed. As the previous case, measurements corresponding to irradiance levels below 800 $\mathrm{W/m^2}$ are excluded in order to decrease the model uncertainty [29], [30]. Compared with the temperature-corrected PR metric, the PVUSA method involves the additional use of wind speed, but is expected to work better especially for technologies with high-temperature coefficients because it takes the effect of wind cooling into account.

IV. Results

Fig. 2 shows the results of the seven methods applied to the module technology c-Si1, where it is possible to notice the main features of the various methods, as described in the previous section: six months missing at the beginning and at the end of the time series for $\mathrm{PR}_{\mathrm{class}}$, high seasonality in all statistical methods, reduction of seasonal effects, and broken time series due to filtering in PVUSA and $\mathrm{PR}_{\mathrm{corr}}$ during winter months.

All results are summarized in Table II and Fig. 3. It can be seen that PV arrays within each technology group defined in Section I show similar behavior in terms of the PLR as well as of the reached confidence interval with the exception of a 1.3% range in the a-Si technologies, which are very different cell architectures ranging from single- to triple-junction designs. Results for CIGS arrays also have a very large divergence (1.9%) mainly due to the very low performance and strong initial degradation of the CIGS3 and CIGS4 arrays. The divergence of 0.8% for crystalline silicon can be attributed to different cell architectures (e.g., back contact) and module types. Interestingly, the behavior within the same technology is clustered around an average value of $-0.7 \pm 0.2\%$ per year for mc-Si (excluding the outlier mc-Si1, which is the array consisting of modules with textured glass. It is possible that this unusually high value of degradation stems from soiling of the texturization; this will be analyzed in future work.), $-0.5 \pm 0.3\%$ per year for c-Si, $-1.7 \pm 0.2\%$ per year for micro, and $-1.4 \pm 0.5\%$ per year for a-Si (simply averaging all arrays using the seven methodologies) (see also Fig. 3). These values are more negative compared with what was reported in [11] based on three years of operation for all technologies using a pure linear regression and the metric

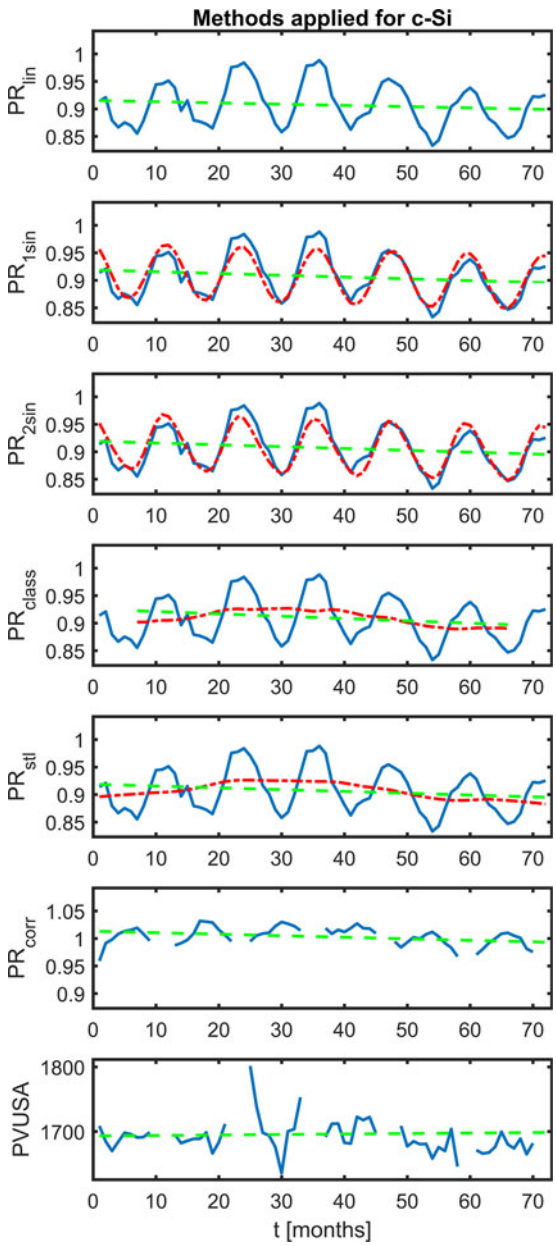

Fig. 2. The methods from top to bottom: linear regression of the uncorrected PR (blue/solid: original data, green/dashed: linear fit), single periodic fitting (blue/solid: original data, red/dot-dashed: fit, green/dashed: linear part of the fit), dual periodic fitting (color/style as above), CSD (blue/solid: original data, red/dot-dashed: long-term trend, green/dashed: linear fit of the trend), STL (color/style as above), PR corrected (blue/solid: PR at STC, green/dashed: linear fit), and PVUSA (blue/solid: metric PVUSA green/dashed: linear fit). PR corrected and PVUSA show missing values in the data in the winter month due to the filtering excluding irradiances below 800 W/m^2. Including lower values will lead to larger errors in the temperature correction for these methods; see [11].

PR. PVUSA seems to be more stable with the extension of the time range from three to six years. When looking at averaged values for the different technologies, one finds the following: $-0.4 \pm 0.4\%$ per year instead of $-0.3 \pm 0.3\%$ per year for c-Si, $-0.85 \pm 0.4\%$ per year instead of $-0.7 \pm 0.3\%$ per year for mc-Si, $-1.2 \pm 0.1\%$ per year instead of $-1.1 \pm 0.7\%$ per year for ribbon, unchanged for micro, 1j-a-Si, and 2j-a-Si. The only relevant differences using PVUSA are to be found in 3j-a-Si and CIGS. Considering only three years of operation, 3j-a-Si showed the positive PLR, and CIGS showed very large negative values that can be attributed to the strong initial degradation of CIGS3 and CIGS4. The influence of the time range and the starting/ending point will be further subject of a deeper analysis and presented in a future work. Another interesting aspect for future analysis is to investigate how different periods (e.g., years, weeks, or even days) over which the PR is computed influence the PLR. Fig. 4 shows the PLR rate with the uncertainties for a single-junction amorphous silicon technology as an example.

Overall, it can be said that all methods produce compatible PLR values for most of the technologies, however with different degrees of uncertainty. With a few exceptions, all applied methods improve the uncorrected computation of the PLR (see Section III-B1).

We find that for the different technologies, the smallest uncertainty can be achieved using the purely statistical method of classical time-series and STL decomposition. In addition, relatively good results can be found using the periodic fitting function, which give similar PLR and uncertainty values. The PVUSA method improves the pure linear regression method, however not to the extent that the other statistical and fitting methods do. The correction of the PR for STC fails to improve the uncertainty and in cases delivers an uncertainty that is even larger than the pure linear regression method (see Fig. 4). In detail, we find the following: for the a-Si technologies, STL reduces the standard deviation on average by half of the standard deviation of the benchmark method, where the corrected PR_{NOCT} enlarges the standard deviation by about 18%, and PVUSA reduces the standard deviation to 88%. In the case of CdTe, no significant reduction was observed. In the case of CIGS, an average reduction to 47% was achieved using STL, whereas PVUSA and PR_{NOCT} enlarge the error by 50%. For micromorph technologies, the STL method reduces the standard deviation to 43% compared to that of the benchmark method. The physical methods enlarge the error by 14% or leave it unaltered. For the crystalline-silicon-based technologies (c-Si and mc-Si), the corrected PR method and the STL method reduce the standard deviation to values between 33% and 45% of the benchmark method, whereas PVUSA reduced the error only to about 45–72%. For the ribbon technology STL, PR_{NOCT} and PVUSA reduce the standard deviation to a third. This can be attributed to the fact that technologies such as the amorphous silicon solar cells have peculiar temperature behavior, in which annealing processes make the cells perform better at elevated temperatures. Additionally, light soaking has an effect on the module's performance. On the whole, the temperature behavior of a-Si PV is not easily describable with a simple temperature coefficient, which makes the correction to STC difficult. A more detailed examination of the temperature coefficient will be presented at the end of this section. In technologies with a large initial degradation like some of the CIGS arrays analyzed in this study, the two series decomposition can produce quite different results. This can be attributed to the fact that, in the classical decomposition, the first six months of the trend are not present.

TABLE II
PLRs (% PER YEAR) WITH UNCERTAINTIES FOR 26 TECHNOLOGIES COMPUTED USING THE SEVEN METHODS DISCUSSED IN THIS PAPER

	PR_{lin}	PR_{1sin}	PR_{2sin}	PR_{class}	PR_{stl}	PR_{NOCT}	PVUSA	Average all
1j-aSi1	-1.5 ± 0.3	-1.5 ± 0.1	-1.4 ± 0.1	-1.4 ± 0.1	-1.4 ± 0.1	-1.6 ± 0.4	-1.4 ± 0.3	-1.5 ± 0.1
1j-aSi2	-1.9 ± 0.3	-1.9 ± 0.2	-1.8 ± 0.1	-1.8 ± 0.1	-1.9 ± 0.1	-2.0 ± 0.4	-1.9 ± 0.3	-1.9 ± 0.1
2j-aSi1	-2.0 ± 0.5	-1.9 ± 0.3	-1.9 ± 0.3	-1.5 ± 0.3	-1.9 ± 0.2	-2.2 ± 0.6	-2.1 ± 0.5	-1.9 ± 0.2
3j-aSi1	-0.8 ± 0.3	-0.8 ± 0.2	-0.8 ± 0.2	-1.0 ± 0.2	-0.8 ± 0.2	-0.9 ± 0.3	-0.8 ± 0.2	-0.8 ± 0.1
3j-aSi2	-0.7 ± 0.3	-0.8 ± 0.2	-0.8 ± 0.2	-1.0 ± 0.2	-0.7 ± 0.2	-0.8 ± 0.3	-0.6 ± 0.2	-0.8 ± 0.1
CdTe2	-1.9 ± 0.1	-1.9 ± 0.1	-1.9 ± 0.1	-1.9 ± 0.1	-1.9 ± 0.1	-1.7 ± 0.1	-1.7 ± 0.1	-1.9 ± 0.1
CIGS2	-2.8 ± 0.1	-2.8 ± 0.1	-2.8 ± 0.1	-3.0 ± 0.1	-2.7 ± 0.1	-2.5 ± 0.2	-2.4 ± 0.1	-2.7 ± 0.2
CIGS3	-4.6 ± 0.3	-4.6 ± 0.3	-4.6 ± 0.3	-4.3 ± 0.1	-4.6 ± 0.2	-5.2 ± 0.4	-4.9 ± 0.5	-4.7 ± 0.3
CIGS4	-3.7 ± 0.2	-3.7 ± 0.2	-3.6 ± 0.2	-3.2 ± 0.1	-3.7 ± 0.2	-3.9 ± 0.3	-3.8 ± 0.3	3.7 ± 0.2
HIT1	-0.7 ± 0.3	-0.9 ± 0.1	-0.9 ± 0.1	-0.9 ± 0.1	-0.9 ± 0.1	-0.8 ± 0.1	-0.8 ± 0.1	-0.8 ± 0.1
c-Si1	-0.3 ± 0.3	-0.4 ± 0.1	-0.4 ± 0.1	-0.5 ± 0.1	-0.4 ± 0.1	-0.3 ± 0.1	0.1 ± 0.2	-0.3 ± 0.2
c-Si2	-0.2 ± 0.4	-0.3 ± 0.1	-0.4 ± 0.1	-0.5 ± 0.1	-0.4 ± 0.1	-0.3 ± 0.1	0.1 ± 0.3	-0.3 ± 0.2
c-Si3	-0.5 ± 0.2	-0.6 ± 0.1	-0.6 ± 0.1	-0.7 ± 0.1	-0.6 ± 0.1	-0.6 ± 0.1	-0.6 ± 0.1	-0.6 ± 0.1
c-Si4	-0.5 ± 0.3	-0.5 ± 0.3	-0.5 ± 0.3	-0.4 ± 0.3	-0.6 ± 0.2	-0.9 ± 0.2	-0.7 ± 0.2	-0.6 ± 0.2
c-Si5	-0.8 ± 0.2	-0.9 ± 0.2	-0.9 ± 0.2	-0.9 ± 0.1	-1.0 ± 0.1	-0.8 ± 0.1	-0.9 ± 0.2	-0.9 ± 0.1
micro1	-1.5 ± 0.2	-1.5 ± 0.1	-1.5 ± 0.1	-1.5 ± 0.1	-1.5 ± 0.1	-1.6 ± 0.2	-1.6 ± 0.2	-1.5 ± 0.1
micro2	-1.9 ± 0.2	-1.9 ± 0.1	-1.9 ± 0.1	-1.8 ± 0.1	-1.9 ± 0.1	-2.1 ± 0.2	-2.0 ± 0.2	-1.9 ± 0.1
micro3	-1.6 ± 0.3	-1.6 ± 0.1	-1.5 ± 0.1	-1.5 ± 0.1	-1.5 ± 0.1	-1.7 ± 0.4	-1.6 ± 0.3	-1.6 ± 0.1
mc-Si1	-2.0 ± 0.3	-2.1 ± 0.1	-2.1 ± 0.1	-2.3 ± 0.1	-2.1 ± 0.1	-1.9 ± 0.1	-1.7 ± 0.2	-2.0 ± 0.2
mc-Si2	-0.6 ± 0.3	-0.7 ± 0.1	-0.7 ± 0.1	-0.8 ± 0.1	-0.7 ± 0.1	-0.7 ± 0.1	-0.8 ± 0.1	-0.7 ± 0.1
mc-Si3	-0.4 ± 0.3	-0.6 ± 0.1	-0.6 ± 0.1	-0.7 ± 0.1	-0.6 ± 0.1	-0.5 ± 0.1	-0.5 ± 0.1	-0.6 ± 0.1
mc-Si6	-0.8 ± 0.2	-0.9 ± 0.1	-0.9 ± 0.1	-0.9 ± 0.1	-0.9 ± 0.1	-0.9 ± 0.1	-0.8 ± 0.1	-0.9 ± 0.1
mc-Si7	-0.9 ± 0.3	-1.0 ± 0.1	-1.0 ± 0.1	-1.1 ± 0.1	-1.0 ± 0.1	-0.9 ± 0.1	-1.0 ± 0.2	-1.0 ± 0.1
mc-Si8	-0.4 ± 0.3	-0.6 ± 0.1	-0.6 ± 0.1	-0.7 ± 0.1	-0.6 ± 0.1	-0.5 ± 0.1	-0.5 ± 0.1	-0.6 ± 0.1
mc-Si9	-0.6 ± 0.3	-0.8 ± 0.1	-0.8 ± 0.1	-0.8 ± 0.1	-0.8 ± 0.1	-0.7 ± 0.1	-0.6 ± 0.1	-0.7 ± 0.1
ribbon1	-1.3 ± 0.3	-1.4 ± 0.1	-1.4 ± 0.1	-1.5 ± 0.1	-1.4 ± 0.1	-1.3 ± 0.1	-1.2 ± 0.1	-1.4 ± 0.1

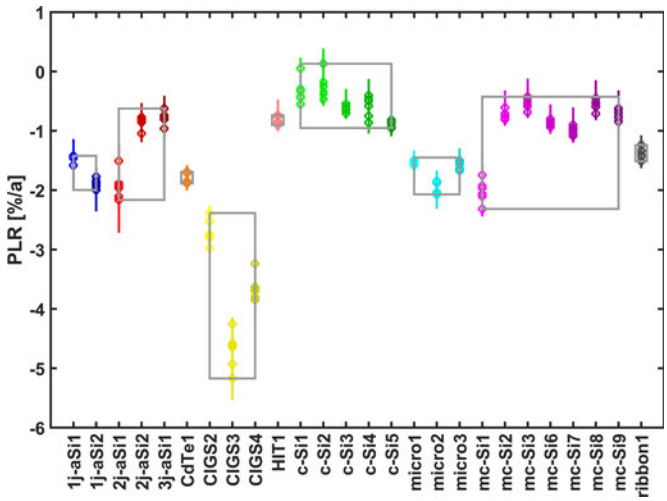

Fig. 3. PLR in percent per year for all technologies. The circles indicate the respective PLR values for the different technologies and methods. The lines indicate the respective errors. The gray boxes are a guide to the eye and show the general range of PLR results for the different technologies. For detailed results, see Table II.

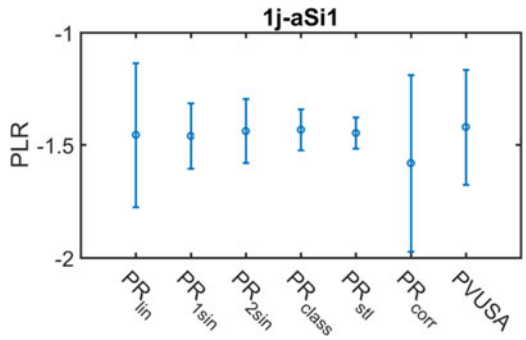

Fig. 4. PLRs for amorphous silicon technologies (example 1j-a-Si1) with the confidence interval of $\pm\sigma$.

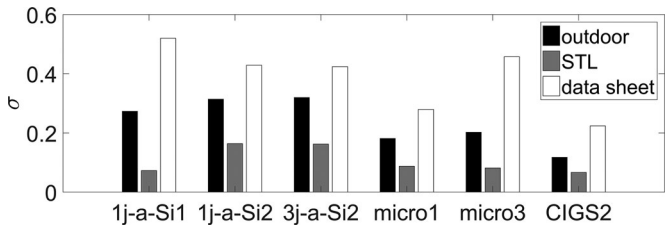

Fig. 5. Black: standard deviation of the PLR computed via the corrected PR method using outdoor temperature coefficients. Gray: standard deviation of the PLR computed using the STL method. White: standard deviation of the PLR computed via the corrected PR method using datasheet temperature coefficients.

For many technologies, the outdoor temperature and seasonal behavior cannot be properly described with only the use of the datasheet power temperature coefficient as other effects dominate over it. An additional study was, thus, performed using results obtained in [48], where outdoor temperature coefficients were calculated using data from the same PV plant described in this current work. In the older study, the datasheet temperature coefficient was compared with outdoor measurements. Phenomenological temperature coefficients were found for different irradiance levels. To further analyze the potential of the PR correction, these outdoor values were used for an irradiation

level of 900 $\mathrm{W/m^2}$. In the crystalline-silicon-based technologies (mc-Si, c-Si, and HIT) and CdTe, the outdoor temperature coefficients are very similar to the datasheet values; hence, no improvement of the PR correction method was achieved. For the other technologies analyzed in [48] (a-Si, micro, CIGS), it was possible to find a moderate improvement in the uncertainty levels. The standard deviation of the PLR determined using the corrected PR was reduced by almost half; however, the uncertainties in no case reached the levels of the STL method (see Fig. 5).

V. Discussions and Conclusion

Overall, STL is the method that consistently produces the lowest or very low uncertainty values. In this method, only the monthly values of the PR are needed, while no knowledge of the technology physics is required because purely statistical methods are used to analyze the long-term trends. CSD performs similarly; however, slightly larger uncertainties are found. This is due to the shorter trend series, which is truncated six months in the beginning and end of the original series. Also satisfying overall results can be reported for the two methods relying on fitting to annual irradiance fluctuations, which do not differ much in terms of uncertainty. It is possible that longer sinusoidal expansions (Fourier-like approach) could deliver even better results, finding a more accurate seasonality.

The methods ($\mathrm{PR_{corr}}$ and PVUSA) that are trying to incorporate the module physics and the influence of module temperature only succeed to reduce the uncertainty if the module/cell temperature behavior is very well understood, i.e., for crystalline-based silicon technologies, such as c-Si, mc-Si, ribbon, and HIT. For the other technologies, other influences such as spectral effects, light soaking, and the temporally delayed effect of high-temperature annealing make it hard to estimate the module production from just the temperature. Other non-monitored effects are more important for these technologies. Trying to resolve this shortcoming using outdoor temperature coefficients does not produce the accuracy found using the time-series decomposition methods, even though the uncertainties were reduced. For the PVUSA and the PR correction methods, another problem arises from the filtering of irradiance only above 800 $\mathrm{W/m^2}$. At the latitude of the PV plant used for the present study, in the winter months, often, there are only very few points to perform the fit to find the parameters defined in Section III-B5. Creating more complex physical models and monitoring more meteorological variables such as module temperature, wind speed, spectrally resolved irradiance, or humidity could improve the correction methods $\mathrm{PR_{NOCT}}$ and PVUSA. However, very few sites that monitor the PV performance are equipped with a spectroradiometer or humidity sensors. Using the statistical methods especially the STL method will enlarge the usable data for performance analysis and even sites that have very little monitoring equipment (only in-plane irradiance and PV power output) will deliver trustworthy performance data. This will open the possibility to explore the PV performance in a wider range of climatic conditions. The results from this study are inline with above-mentioned study by Phinikarides *et al.* [37]. In the future, we plan to compare the proposed methods on a more general level and use data from other sites in other climate zones.

In conclusion, it can be said that, as the temperature behavior of non-crystalline-silicon-based technologies is hard to predict, it is favorable to use purely statistical methods to reduce the seasonal fluctuation for these technologies. To keep the PLRs comparable between all technologies, it is advisable to use one method for all technologies. We propose the use of statistical methods such as STL over the deterministic methods, for all technologies to find the PLR to be included into international standards for the determination of the PLR. In addition to this, it is also important to stress the need of an agreed methodology for the calculation of the PLR and on the definition of absolute $(12a)$ and relative $(12a/b)$ PLR. While the power of the first definition lies in the fact that it can be directly applied on the PR values, the latter can be used to any metrics where the initial value is known, e.g., energy yield, efficiency, etc. Thus, the relative PLR should be used when considering business models or long-term efficiency studies, as the relative PLR is more easily generalized to these cases. In any case, the recommendation is to clearly state when the PLR is calculated in absolute or relative terms.

Acknowledgment

The authors would like to thank the Stiftung Südtiroler Sparkasse for co-funding the activities within the IEA-PVPS Task 13 network. The authors thank the Department of Innovation, Research and University of the Autonomous Province of Bozen/Bolzano for covering the Open Access publication costs.

References

[1] *Renewable Capacity Statistics 2017*, Int. Renewable Energy Agency, Abu Dhabi, UAE, 2017.

[2] U. Jahn, D. Moser, and M. Richter, "Minimizing Technical Risks in PhotovoltaicProjects, Recommendations for Minimizing Technical Risks of PV Project Development and PV Plant Operation—EU Horizon 2020 Project: Solar Bankability—Delivery Report," Tech. Rep., 2016. [Online]. Available: http://www.solarbankability.org/fileadmin/sites/www/files/documents/Solar_Bankability_D1.2_2.2_MitigationMeasures_Final_Version.pdf

[3] T. Huld, E. Dunlop, H. G. Beyer, and R. Gottschalg, "Data sets for energy rating of photovoltaic modules," *Sol. Energy*, vol. 93, pp. 267–279, 2013.

[4] D. Dirnberger, G. Blackburn, B. Müller, and C. Reise, "On the impact of solar spectral irradiance on the yield of different PV technologies," *Sol. Energy Mater. Sol. Cells*, vol. 132, pp. 431–442, 2015.

[5] *Photovoltaic (PV) Module Performance Testing and Energy Rating—Part 1: Irradiance and Temperature Performance Measurements and Power Rating*, IEC61853-1:2011, 2011.

[6] *Photovoltaic (PV) Module Performance Testing and Energy Rating—Part 2: Spectral Responsivity, Incidence Angle and Module Operating Temperature Measurements* , IEC61853-2:2011, 2011.

[7] A. Ndiaye *et al.*, "Degradations of silicon photovoltaic modules: A literature review," *Sol. Energy*, vol. 96, pp. 140–151, 2013.

[8] M. Quintana, D. King, T. McMahon, and C. Osterwald, "Commonly observed degradation in field-aged photovoltaic modules," in *Proc. 29th IEEE Photovoltaic Spec. Conf.*, New Orleans, LA, USA, 2002, pp. 1436–1439.

[9] M. Köntges *et al.*, "Review of failures of photovoltaic modules," Tech. Rep. IEA-PVPS T13-01:2014, IEA, Paris, France, 2013.

[10] V. Sharma and S. S. Chandel, "Performance and degradation analysis for long term reliability of solar photovoltaic systems: A review," *Renewable Sustain. Energy Rev.*, vol. 27, pp. 753–767, 2013.

[11] G. Belluardo *et al.*, "Novel method for the improvement in the evaluation of outdoor performance loss rate in different PV technologies and comparison with two other methods," *Sol. Energy*, vol. 117, pp. 139–152, 2015.
[12] A. J. Carr and T. L. Pryor, "A comparison of the performance of different PV module types in temperate climates," *Sol. Energy*, vol. 76, no. 1–3, pp. 285–294, 2004.
[13] D. Polverini, M. Field, E. Dunlop, and W. Zaaiman, "Polycrystalline silicon PV modules performance and degradation over 20 years," *Prog. Photovoltaics, Res. Appl.*, vol. 21, no. 5, pp. 1004–1015, 2013.
[14] N. Kahoul, M. Houabes, and M. Sadok, "Assessing the early degradation of photovoltaic modules performance in the Saharan region," *Energy Convers. Manage.*, vol. 82, pp. 320–326, 2014.
[15] M. A. Munoz, M. C. Alonso-Garcia, N. Vela, and F. Chenlo, "Early degradation of silicon PV modules and guaranty conditions," *Sol. Energy*, vol. 85, no. 9, pp. 2264–2274, 2011.
[16] A. Ndiaye *et al.*, "Degradation evaluation of crystalline-silicon photovoltaic modules after a few operation years in a tropical environment," *Sol. Energy*, vol. 103, pp. 70–77, 2014.
[17] G. Makrides, B. Zinsser, M. Schubert, and G. E. Georghiou, "Performance loss rate of twelve photovoltaic technologies under field conditions using statistical techniques," *Sol. Energy*, vol. 103, pp. 28–42, 2014.
[18] A. Kamei, S. Yoshida, H. Takakura, and T. Minemoto, "Ten years outdoor operation of silicon based photovoltaic modules at central latitude of Japan," *Renewable Energy*, vol. 65, pp. 78–82, 2014.
[19] D. C. Jordan, S. R. Kurtz, K. VanSant, and J. Newmiller, "Compendium of photovoltaic degradation rates," *Prog. Photovoltaics, Res. Appl.*, vol. 24, no. 7, pp. 978–989, Jul. 2016. [Online]. Available: http://onlinelibrary.wiley.com/doi/10.1002/pip.2744/abstract
[20] D. Jordan, J. Wohlgemuth, and S. Kurtz, "Technology and climate trends in PV module degradation," in *Proc. 27th Eur. Photovoltaic Sol. Energy Conf. Exhib.*, Frankfurt, Germany, 2012, pp. 3118 –3124.
[21] A. Skoczek, T. Sample, and E. D. Dunlop, "The results of performance measurements of field-aged crystalline silicon photovoltaic modules," *Prog. Photovoltaics, Res. Appl.*, vol. 17, no. 4, pp. 227–240, 2009.
[22] D. C. Jordan and S. R. Kurtz, "Photovoltaic degradation rates-an analytical review," *Prog. Photovoltaics, Res. Appl.*, vol. 21, no. 1, pp. 12–29, 2013.
[23] M. Kendall, *Time-Series*, 2nd ed. London, U.K.: Griffin, 1976.
[24] R. J. Hyndman and G. Athanasopoulos, *Forecasting: Principles and Practice*. Melbourne, Australia: OTexts, 2013. [Online]. Available: http://otexts.org/fpp/, Accessed on: Jan. 16, 2017.
[25] R. B. Cleveland, W. S. Cleveland, J. E. McRae, and I. Terpenning, "STL: A seasonal-trend decomposition procedure based on loess," *J. Official Statist.*, vol. 5, no. 1, pp. 3–33, Jan. 1990. [Online]. Available: https://www.scienceopen.com/document?vid=be074647-46c0-4ba9-991e-3124fbf63ed1
[26] J. Chambers, W. Cleveland, and B. Kleiner, *Graphical Methods for Data Analysis*. Belmont, CA, USA: Wadsworth, 1983.
[27] D. Bartholomew, G. Box, and G. Jenkins, "Time series analysis forecasting and control," *Oper. Res. Quart.*, vol. 22, no. 2, pp. 199–201, 1971.
[28] M. Nikolaeva-Dimitrova, R. P. Kenny, E. D. Dunlop, and M. Pravettoni, "Seasonal variations on energy yield of a-Si, hybrid, and crystalline Si PV modules," *Prog. Photovoltaics, Res. Appl.*, vol. 18, no. 5, pp. 311–320, 2010. [Online]. Available: http://onlinelibrary.wilaey.com/doi/10.1002/pip.918/abstract
[29] G. Makrides, B. Zinsser, G. Georghiou, M. Schubert, and J. Werner, "Degradation of different photovoltaic technologies under field conditions," in *Proc. 35th IEEE Photovoltaic Spec. Conf.*, Honolulu, HI, USA, 2010, pp. 2332–2337.
[30] D. Jordan, R. Smith, C. Osterwald, E. Gelak, and S. Kurtz, "Outdoor PV degradation comparison," in *Proc. 35th IEEE Photovoltaic Spec. Conf.*, Honolulu, HI, USA, 2010, pp. 2694–2697.
[31] A. Kimber *et al.*, "Improved test method to verify the power rating of a photovoltaic (PV) project," in *Proc. 34th IEEE Photovoltaic Spec. Conf.*, 2009, pp. 316–321.
[32] S. A. Pethe, A. Kaul, and N. G. Dhere, "Statistical data analysis of thin film photovoltaic modules deployed in hot and humid climate of Florida," *Proc. SPIE*, vol. 7048, 2008, Art. no. 70480T.
[33] D. C. Jordan, M. G. Deceglie, and S. R. Kurtz, "PV degradation methodology comparison—A basis for a standard," in *Proc. IEEE 43rd Photovoltaic Spec. Conf.*, 2016, pp. 273–278.
[34] A. Kyprianou, A. Phinikarides, G. Makrides, and G. E. Georghiou, "Definition and computation of the degradation rates of photovoltaic systems of different technologies with robust principal component analysis," *IEEE J. Photovoltaics*, vol. 5, no. 6, pp. 1698–1705, Nov. 2015.
[35] A. Phinikarides, G. Makrides, B. Zinsser, M. Schubert, and G. E. Georghiou, "Analysis of photovoltaic system performance time series: Seasonality and performance loss," *Renewable Energy*, vol. 77, pp. 51–63, 2015.
[36] D. C. Jordan and S. R. Kurtz, "Analytical improvements in PV degradation rate determination," in *Proc. 35th IEEE Photovoltaic Spec. Conf.*, 2010, pp. 2688–2693.
[37] A. Phinikarides, N. Kindyni, G. Makrides, and G. E. Georghiou, "Review of photovoltaic degradation rate methodologies," *Renewable Sustain. Energy Rev.*, vol. 40, pp. 143–152, 2014.
[38] G. Belluardo, M. Pichler, D. Moser, and M. Nikolaeva-Dimitrova, "One-year comparison of different thin film technologies at Bolzano airport test installation," in *Fuelling the Future: Advances in Science and Technologies for Energy Generation, Transmission and Storage*, A. Mendez-Vilas, Eds. Irvine, CA, USA: Brown Walker Press, 2012.
[39] M. C. Peel, B. L. Finlayson, and T. A. McMahon, "Updated world map of the Köppen-Geiger climate classification," *Hydrol. Earth Syst. Sci.*, vol. 11, no. 5, pp. 1633–1644, 2007. [Online]. Available: http://www.hydrol-earth-syst-sci.net/11/1633/2007/
[40] S. I. A. |. I. A. A. SPA, "Historical Data | Weather | Autonomous Province of Bozen/Bolzano." [Online]. Available: http://weather.provinz.bz.it/historical-data.asp, Accessed on: Aug. 28, 2017.
[41] L. Fanni, M. Giussani, M. Marzoli, and M. Nikolaeva-Dimitrova, "How accurate is a commercial monitoring system for photovoltaic plant?" *Prog. Photovoltaics, Res. Appl.*, vol. 22, no. 8, pp. 910–922, 2014.
[42] D. Bertani, S. Guastella, G. Belluardo, and D. Moser, "Long term measurement accuracy analysis of a commercial monitoring system for photovoltaic plants," in *Proc. IEEE Workshop Environ., Energy, Struct. Monit. Syst.*, 2015, pp. 84–89.
[43] *Photovoltaic System Performance Monitoring Guidelines for Measurement, Data Exchange, and Analysis*, IEC61724:1998, 1998.
[44] *Curve Fitting Toolbox User's Guide*, The MathWorks, Inc., Natick, MA, USA, 2015. [Online]. Available: https://www.mathworks.com/help/pdf_doc/curvefit/curvefit.pdf
[45] A. Trapletti and K. Hornik, *Tseries: Time Series Analysis and Computational Finance*, R package version 0.10-38, 2017. [Online]. Available: https://CRAN.R-project.org/package=tseries
[46] R Core Team, *R: A Language and Environment for Statistical Computing*, R Foundation for Statistical Computing, Vienna, Austria, 2013. [Online]. Available: http://www.R-project.org/
[47] C. Whitaker *et al.*, "Application and validation of a new PV performance characterization method," in *Proc. 26th IEEE Photovoltaic Spec. Conf.*, Anaheim, CA, USA, 1997, pp. 1253–1256.
[48] D. Moser, M. Pichler, and M. Nikolaeva-Dimitrova, "Filtering procedures for reliable outdoor temperature coefficients in different photovoltaic technologies," *J. Sol. Energy Eng.*, vol. 136, no. 2, 2013, Art. no. 21006.

Authors' photographs and biographies not available at the time of publication.